Available online at www.sciencedirect.com
SCIENCE DIRECT
Tetrahedron 62 (2006) 4900–4906
Tetrahedron

Nanoarchitecture self-assembly and photochromic studies of 2,2-diarylnaphthopyrans

Ting-Feng Tan,[a] Jie Han,[a] Mei-Li Pang,[a] Yi-Fang Fu,[a] Hong Ma,[b] Yu-Xin Ma[a] and Ji-Ben Meng[a,*]

[a]*Department of Chemistry, Nankai University, Tianjin 300071, People's Republic of China*
[b]*Department of Materials Science and Engineering, University of Washington, Seattle, WA 98195, USA*

Received 2 December 2005; revised 27 February 2006; accepted 2 March 2006
Available online 27 March 2006

Abstract—The synthesis and photochromic properties of novel 2,2-diarylnaphthopyrans were described. Significantly, the nanostructured architecture through two-component self-assembly of a photochromic naphthopyran and an asymmetric biphenyl was determined by X-ray diffraction. The structure motifs of nanocavities were formed by Cl···O interactions and Ar–H···Cl hydrogen bonds among the photochromic naphthopyran molecules. It was further shown by TEM that the dimensions of cavity structures were up to nanometer level, which provides the potential to capture useful nanoscale entities and control photochromism in organic materials.

1. Introduction

The design and synthesis of photochromic molecules is an intense research area because of their potential applications in optical memory, photo-optical switching, and nonlinear optics.[1–6] Naphthopyrans are one of the most studied and important class of photochromic compounds.[7,8] Nowadays, it is possible to obtain any color using only naphthopyrans.[9] Owing to their good photochromic properties, associated with high fatigue resistance, naphthopyrans have been used in the manufacture of photochromic lenses that darken in sunlight.[10] This photochromic behavior is based on a photoinduced reversible opening of the pyran ring that converts the colorless form (closed form) into the isomers (opened form).[8] The observation of a distinct absorption spectrum is due to the extensively π-conjugated system present in the opened form.[11]

Quite few self-assembly of photochromic molecules were reported. In this paper, we intended to report the preparation of a new series of photochromic 2,2-diarylnaphthopyrans **1**–**6** (Scheme 1) and the study of their photochromic behaviors in various media including organic solvents and polymethyl methacrylate (PMMA). Significantly, the nanostructured architecture was realized through two-component self-assembly of a photochromic naphthopyran and an asymmetric biphenyl in the crystal. It was further shown by TEM that the dimensions of cavity structures were up to nanometer level, which provided the potential to capture useful nanoscale entities and control photochromism in organic

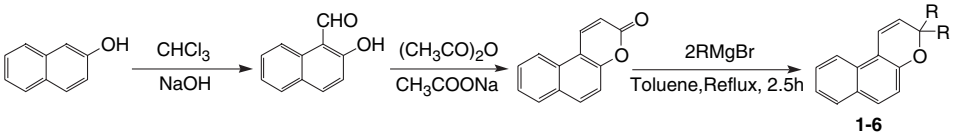

Scheme 1. Routine of synthesis of 2,2-diarylnaphotopyrans derivatives **1**–**6** where R=3-CF_3–C_6H_4, 4-$(CH_3)_3C$–C_6H_4, 4-CH_3S–C_6H_4, 2,4-dimethoxy-1-phenyl, 3-F-4-CH_3O–C_6H_3, and 3-Cl-4-CH_3O–C_6H_3.

Supplementary data associated with this article can be found in the online version at doi:10.1016/j.tet.2006.03.003.
Keywords: Nanoarchitecture; Self-assembly; Photochromism; 2,2-Diarylnaphthopyrans; PMMA.
* Corresponding author. Tel.: +86 2223 509 933; fax: +86 2223 502 230; e-mail: mengjiben@nankai.edu.cn

0040–4020/$ - see front matter © 2006 Elsevier Ltd. All rights reserved.
doi:10.1016/j.tet.2006.03.003

materials. We are presently exploring a method of replacing the guests by other biphenyls or dipyridines.

2. Results and discussion

2.1. X-ray crystal structural studies

The X-ray crystal structures of 2,2-diarylnaphthopyrans **3** (R=4-CH_3S–C_6H_4) were presented in Figure 1a. An asymmetric unit consisted of two molecules in the compound **3** (CCDC 258742). The packing of molecules (b) in compound **3** were given in Figure 1b. The crystals were monoclinic, in space group $P2_1$. Compound **3** exhibited 2-D supramolecular structures, as illustrated in Figure 1b. An extended zigzag tape was generated via C1–H1···S3 and C47–H47A···S4. Recrystallization of compound **4** (R=2,4-dimethoxy-phenyl) from ethanol yielded a clathrate with ethanol as guest. The packing structure of compound **4** (CCDC 258582), given in Figure 2, displayed a nanometer cavity structure.[12]

2.2. Nanoarchitecture self-assembly

As shown in Figure 3, compound **6** yielded the clathrate with an asymmetric biphenyl **I** from ethanol solution (CCDC 272162). The two phenyl rings themselves and naphtho moiety itself of molecule **6** in the crystal were approximately planar and dihedral angles were 75.0° between the naphtho ring and one phenyl (Ph) group (C14C15C16C17C18C19), and 61.3° between the naphtho ring and the other one (C21C22C23C2C25C26), respectively. Moreover, the dihedral angle between two phenyl rings themselves of compound **6** was 89.0°.

The substituent groups on the phenyl rings of molecule **6** had an insignificant effect on the length of the C_{sp^3}−O bond and on the nonplanarity of the pyran ring. It was shown in Figure 3 that the pyran ring was nonplanar, with folding along the O1···C11 and O1···C12 axes. The dihedral angle was 23.1° between the O1/C13/C12 and O1/C12/C11 planes, and 12.7° between the O1/C12/C11 and O1/C11/C10 planes, while the corresponding values in 3,3-(1-phenyl)-3*H*-naphtho[2,1-*b*]pyran were 22.9 (2) and 10.0 (2)°, respectively.[13]

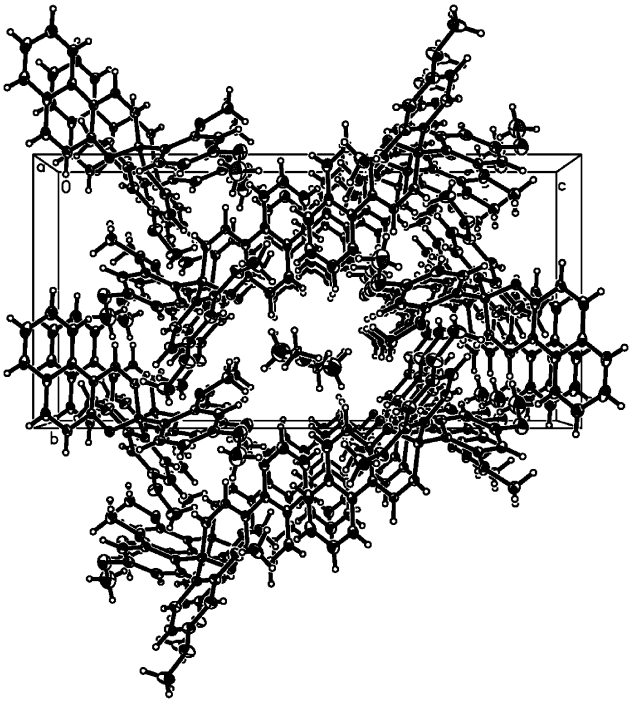

Figure 2. Packing of molecules of compound **4**.

A weak C13–O1 bond was confirmed by the X-ray diffraction data. The bond length was 1.465 (5) Å and was longer than the normal C–O bond (1.41–1.43 Å)[14] in six-member heterocycle, but this kind of change was coincident with other spiro compounds. The angles of the C_{sp^3}−O bond with the Ph ring planes (C14C15C16C17C18C19) and (C21C22C23C24C25C26) were 54.5 and 67.8°, respectively.

The crystal structure of the clathrate (Fig. 4) exhibited the molecules of **6** to form a centrosymmetric dimer in the cell with a space group of *C*2/*c*. Weak Cl···O (3.182 Å) interactions and Ar–H···Cl (2.906 Å) hydrogen bonds linked the

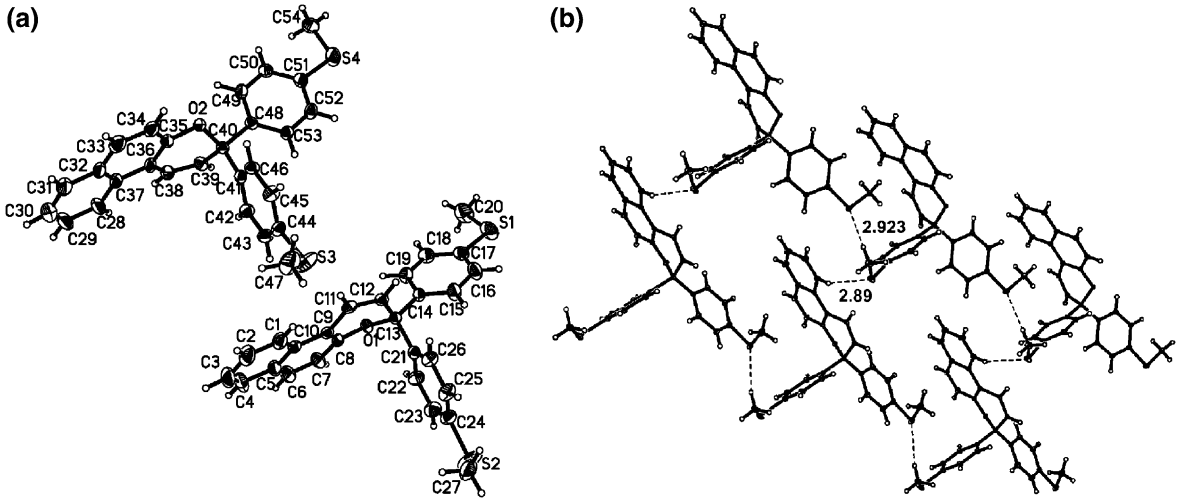

Figure 1. X-ray crystallographic structure (a) and packing of molecules (b) of compound **3**.

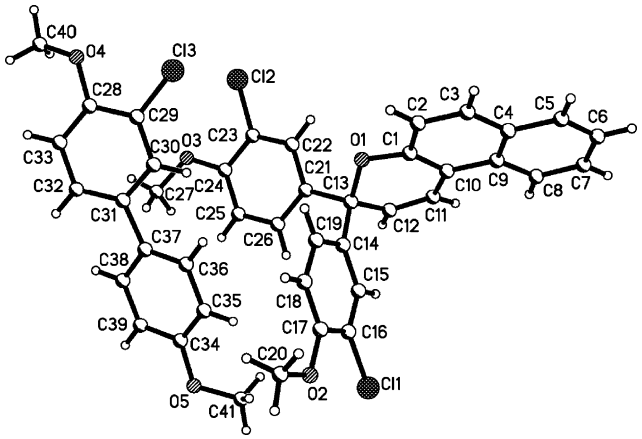

Figure 3. The self-assembled structure of molecules **6** and **I**.

two host molecules, and Ar–H···Cl (2.752 Å) hydrogen bond linked the host–guest molecule. As shown in Figure 4, the clathrate of **6** and **I** in their crystal from ethanol had host–guest stoichiometry of 4:1.

The crystal packing of molecule **6** showed nanostructured cavities along the *b* axis (Fig. 5) with the dimensions of 15.9×8.5 Å and 3.6×8.5 Å, respectively. The potential of these cavities to capture useful nanoscale entities and control photochromism in crystals are currently being explored.

Partial lattice voids were occupied by the protruding chloro groups of the helicene host molecules, so that an alternating arrangement of guest and substituents occurs. The molecular conformation of compound **I** in its crystal and the packing space filling representations of compound **I** and **6** were shown in Figure 6 and Figure 7, respectively.

2.3. TEM image of compound 6

Compound **6** was ground and dissolved in ethanol, then volatilized into a film for TEM image. Crystal morphology of compound **6** was studied by TEM on Philip FEI TECNAI-20. TEM image of photochromic compound **6** was shown in Figure 8, which verified that the whole arrangement of molecular self-assembly was of cavity structure in the crystal. To our surprise, the dimension of cavity structure determined by TEM was up to nanometer level, which is rarely found in organic compounds. It would be of great use for the molecular assembly suggesting the opportunities for inclusion complex formation.

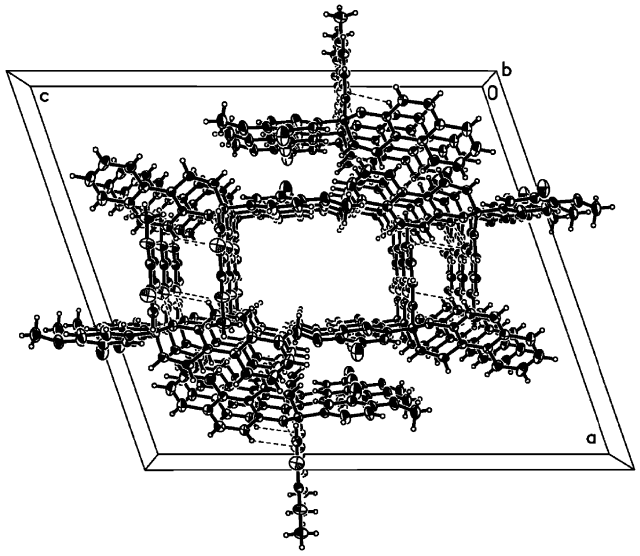

Figure 5. Crystal packing diagram of compound **6** along *b* axis.

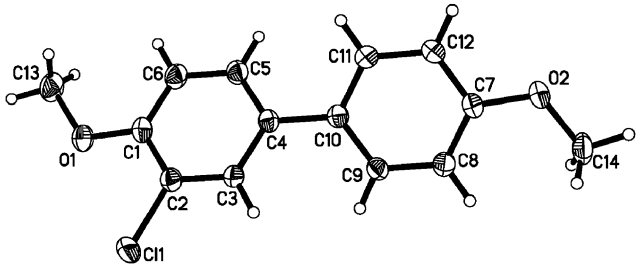

Figure 6. The molecular structure of compound **I**.

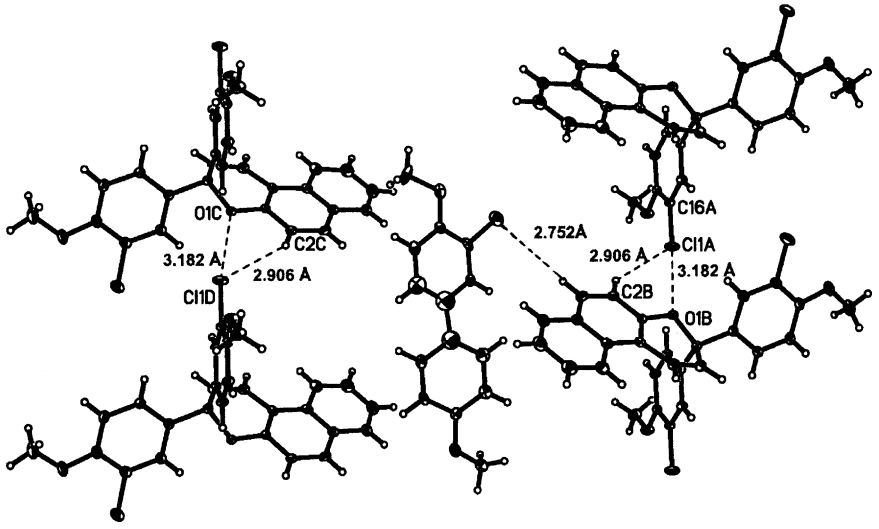

Figure 4. Packing excerpt of helicene compound **6** and **I** (4:1) with Cl···O and Ar–H···Cl contacts (dashed lines) along the *a* axis.

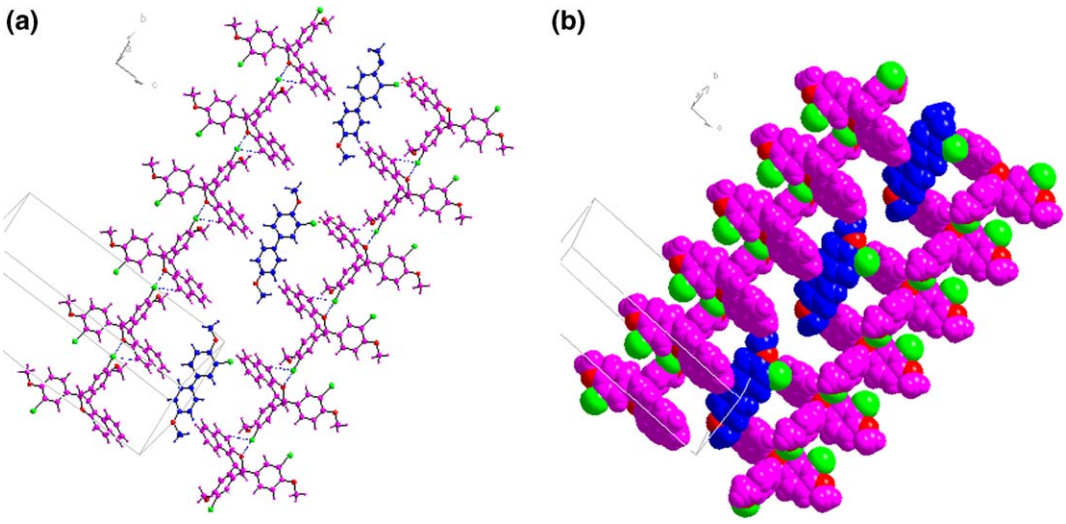

Figure 7. The packing stick (a) and space filling representations (b) of compound **6** and **I**.

2.4. Photochromic properties

The nanostructural assemblies had some influence on the photochromic properties of this series. Compound **6** yielded the clathrate with an asymmetric biphenyl **I** from ethanol solution. The nanostructural assembly is carried out in crystalline state. Although visible color change is observed with the naked eye in crystalline state, photochromism in crystalline state cannot be tested in the existing experimental circumstances.

The absorption spectra of compounds **1**–**6** were observed in solution. It was noteworthy that an obvious color change occurred on irradiation by UV-light or sunlight. Upon excitation at 365 nm, compounds **1**–**6** exhibit photochromic behaviors at room temperature in chloroform, with a visible absorption band at 409–498 nm, corresponding to the generation of the open ring form (Table 1). As shown in Figure 9, upon excitation at 365 nm, compound **4** in chloroform solution exhibited excellent photochromism, with a strong absorption band at 483 nm, resulting from the generation of the open ring form. The open ring form is thermally unstable and readily undergoes thermal bleaching, which follows first-order kinetics, to the ring-closed form.

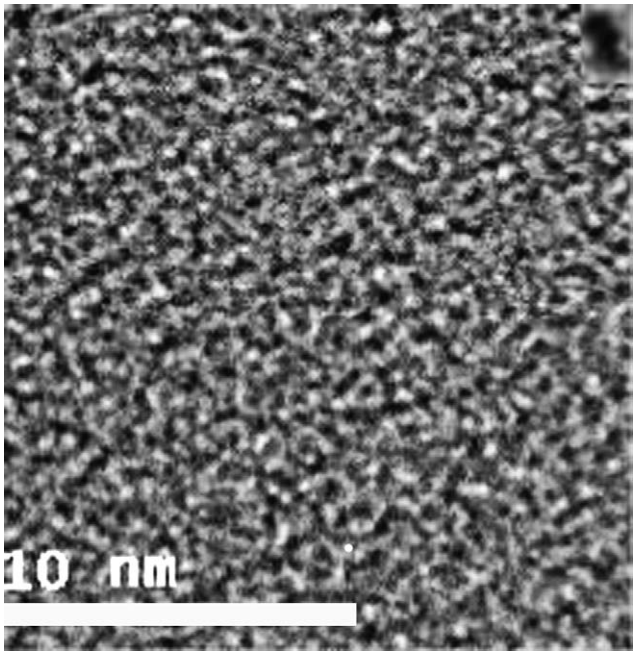

Figure 8. TEM image of the crystal of photochromic compound **6**.

Table 1. The maximum absorption wavelength (λ_{max}) of compounds **1**–**6** in chloroform solution (10^{-5} mol/L) after UV–vis irradiation

Compd	Irradiation time (s)	λ_{max} in solution (nm)	Absorption intensity
1	60	409	0.20
2	60	469	0.21
3	60	498	0.05
4	30	483	1.02
5	60	443	0.04
6	30	473	0.19

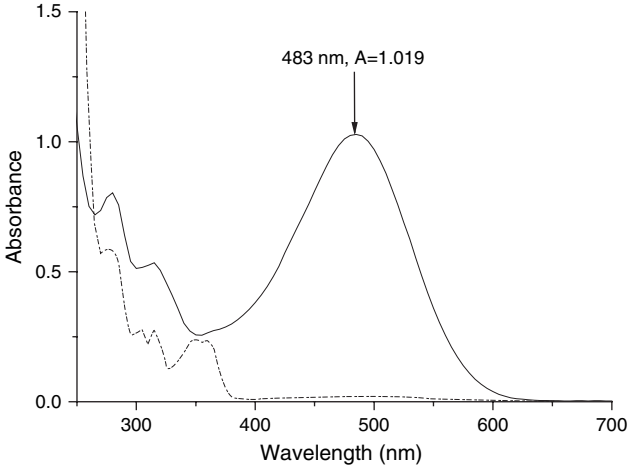

Figure 9. UV–vis absorption spectra of compound **4** before (·····) and after (——) in acetone.

2.4.1. Absorption spectra in polymer films. Films of all species were prepared (2 wt % loading) in PMMA with 1 μm thickness. The state of these compounds in PMMA

Table 2. The maximum absorption wavelength (λ_{max}) of compounds **1**–**6** in PMMA films (2 wt % loading) after UV–vis irradiation

Compd	Irradiation time	λ_{max} in PMMA film (nm)	Absorption intensity	$t_{A_0/2}$ (min)
1	60	409	0.10	170
2	60	450	0.09	160
3	60	479	0.06	140
4	30	486	1.25	670
5	60	465	0.07	150
6	30	463	0.10	170

was amorphous without self-assembly. The absorbance of each film at its λ_{max} was recorded immediately after irradiation for 30 s at 365 nm with a 12 W ultraviolet lamp. Upon excitation at 365 nm, compounds **1**–**6** exhibited photochromic behaviors at room temperature in PMMA, with a visible absorption band at 409–486 nm, corresponding to the generation of the open ring form (Table 2). The absorption intensities of compounds **1**, **2**, **3**, **5**, and **6** at the maximum wavelength in films after UV–vis irradiation were small, but that of **4** was large. In the discussion below, we only described the films of **4** and **6**. The coloration and bleaching of **4** (a) and **6** (b) following irradiation were shown in Figure 10.

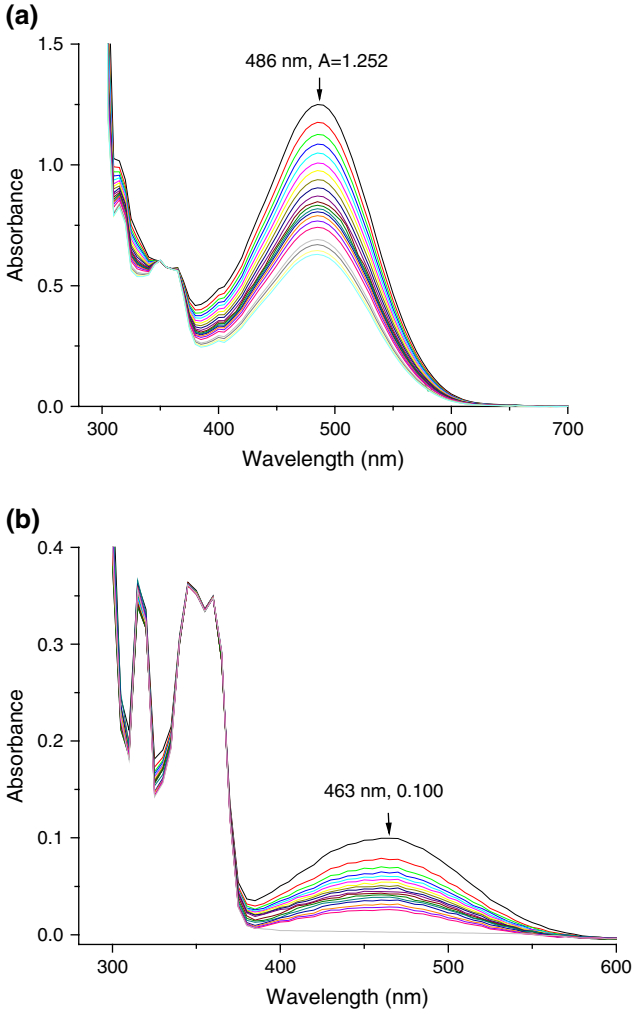

Figure 10. Absorption spectra of compounds **4** (a) and **6** (b) in PMMA films after irradiation at 365 nm with a 12 W ultraviolet lamp for 30 s at different decay times.

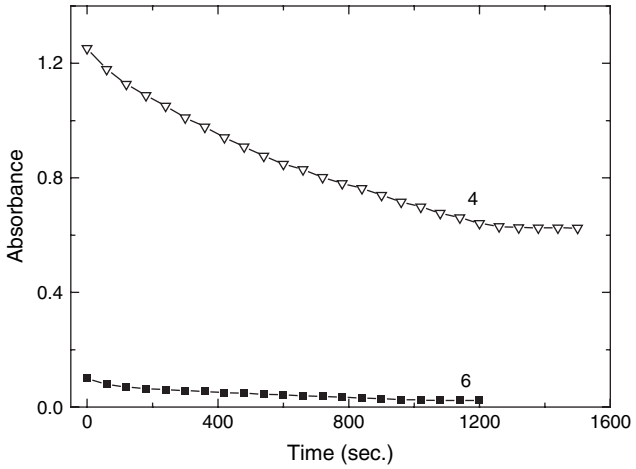

Figure 11. Absorption changes at the λ_{max} of **4** (▽) and **6** (■) in PMMA during the decoloration process at room temperature after the irradiation at 365 nm with a 12 W ultraviolet lamp.

Figure 2 showed that the representative UV–vis absorption spectra changed in the photomerocyanines with time. Following UV–vis irradiation for 30 s, a new absorption band appeared with a maximum absorption wavelength of **4** at 486 nm or **6** at 463 nm, which demonstrated that they exhibited excellent photochromism.

The two-methoxy substituents in the phenyl ring led to red shifts of the absorption band and the electron-donor groups stabilized the open-ring isomers.[15] The photochromic performance is based on the photoinduced reversible opening of the pyran ring as described in the literature.[16]

The thermally reversible processes of compounds **4** and **6** in PMMA films were studied by plotting absorbances at the same λ_{max} for a given compound at different time. A typical example of the plot made for compounds **4** and **6** was illustrated in Figure 11. As shown in Figure 3, the intensity of absorption band at its λ_{max} was decreased gradually during the decoloration process.

2.4.2. The parameter $t_{A_0/2}$ for the fatigue resistance in PMMA films. Sixteen slices of thin-films of **4** and **6** (2 wt % loading) in PMMA were prepared, respectively. All films were irradiated at the same time with a 400 W high-pressure mercury lamp. The absorbances at the λ_{max} of a given compound at different irradiation time were recorded on a spectrophotometer immediately after irradiation. A plot of the absorbance against the irradiation time was given in Figure 12. The parameter $t_{A_0/2}$ obtained from the plot is defined as the required time in minute decreasing the initial absorbance (A_0) at the λ_{max} of the merocyanine form to the half value ($A_0/2$). As shown in Table 2, the $t_{A_0/2}$ of **4** was calculated to be 670 min, and the $t_{A_0/2}$ of **6** was 170 min through a linear extrapolation of the data.[17] It seemed that electron donors increased the lifetime of the open ring form.

2.4.3. Evaluation of the fatigue resistance of 4 in PMMA films. PMMA film was irradiated with a 12 W ultraviolet lamp. The absorbances at λ_{max} of compound **4** were recorded on a spectrophotometer immediately before and after UV

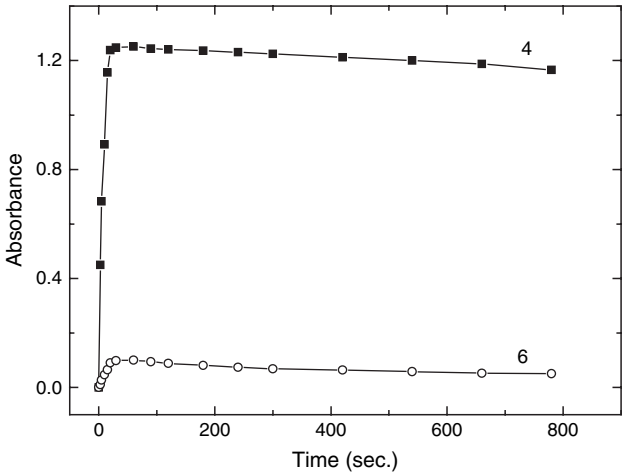

Figure 12. The absorption changes at the λ_{max} of **4** (λ_{max} =486 nm, 2 wt % loading) and **6** (λ_{max}=463 nm, 2 wt % loading) in PMMA films under continuous UV–vis irradiation with a 400 W high-pressure mercury lamp.

irradiation in a 40-time cycle. The absorbances at λ_{max} were zero before UV irradiation (ring-closed form), but they were different after UV irradiation (ring-opened form). On gradual increase of cycle times, the absorbances at λ_{max} were gradually decreased after UV irradiation (ring-opened form). A plot of the absorbance against the cycle times was made as shown in Figure 13. The fatigue resistance was examined after 280-cycle irradiation of UV–vis. As shown in Figure 13, the fatigue resistance of compound **4** was examined and recorded. After 280-cycle UV–vis irradiation, the absorbance at maximum wavelength was kept in 99.1% of that of first irradiation in open ring form. As it was extrapolated to 1000 cycles, the absorbance of maximum wavelength after UV–vis irradiation would be kept in 96.9% of that of first irradiation in open ring form ($A=A_0(1-X)^n$, where n: cycle times, A_0: the original absorption intensity; X: the variational absorption intensity). It was shown that 2,2-diarylnaphthopyrans exhibited excellent stability. The useful lifetime of the photochromic films is of utmost importance to its commercial success.

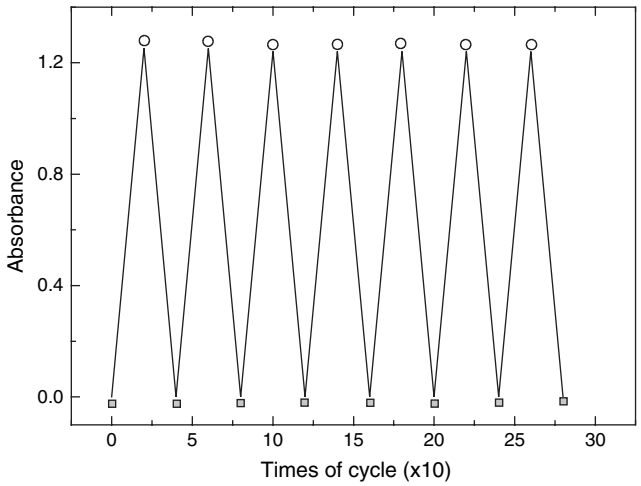

Figure 13. Photoinduced absorption changes for compound **4** in PMMA film at λ_{max}; photoirradiation started at each point of □ with visible light, finished at the point of ○ and started with UV light.

3. Experimental

3.1. General procedure for the synthesis of 2,2-diarylnaphthopyrans (entries 1–6)

The target compounds **1**–**6** were prepared in moderate yields through reactions of Grignard reagents with naphthopyran biones in dry tetrahydrofuran (THF) instead of toluene.[18–20]

Prepared Grignard reagent (10 mmol) in diethyl ether was added to naphthopyran bione (5 mmol, synthesized as described in the literature[18]) in dry THF under reflux.[19,20] The mixtures were stirred until no starting materials remained in TLC. The reaction mixture was then cooled to room temperature and ethyl ether was added to extract the organic layer. The organic phases were combined, and dried with anhydrous magnesium sulfate. Solvent evaporation gave a crude product, which was purified by a silica-gel column chromatography using petroleum ether/ethyl ether as eluent. Recrystallization from ethanol or acetone gave a crystalline material.

3.1.1. 2,2-Bis(3-trifluoro methylphenyl)-3*H*-naphtho[2,1-*b*]pyran (1). Yield: 46%. Mp: 103–104 °C. ^{1}H NMR: δ 6.21 (d, 1H, J=6.6 Hz), 7.14–7.43 (m, 14H), 7.75 (d, 1H, J=6.0 Hz). IR (KBr): 1622, 1510 (C=C) cm^{-1}, 1330, 1224 (C–F) cm^{-1}. EIMS: m/z 471 (M^+). Anal. Calcd for $C_{27}H_{16}F_6O$: C, 68.94; H, 3.40. Found: C, 68.70; H, 3.41.

3.1.2. 2,2-Bis(4-tertiary butylphenyl)-3*H*-naphtho[2,1-*b*]pyran (2). Yield: 36%. Mp: 194–195 °C. ^{1}H NMR: δ 1.27 (s, 18H), 6.28 (d, 1H, J=6.6 Hz), 7.20–7.72 (m, 14H), 7.93 (d, 1H, J=5.4 Hz). IR (KBr): 2962, 1463, 1361 (C=C) cm^{-1}. EIMS: m/z 447 (M^+). Anal. Calcd for $C_{33}H_{34}O$: C, 88.79; H, 7.62. Found: C, 88.51; H, 7.61.

3.1.3. 2,2-Bis(4-sulfur methylphenyl)-3*H*-naphtho[2,1-*b*]pyran (3). Yield: 36%. Mp: 142–143 °C. ^{1}H NMR: δ 2.43 (s, 6H), 6.17 (d, 1H, J=6.6 Hz), 7.14–7.71 (m, 14H), 7.93 (d, 1H, J=5.6 Hz). IR (KBr): 1618, 1510 (C=C) cm^{-1}. EIMS: m/z 427 (M^+). Anal. Calcd for $C_{27}H_{22}OS_2$: C, 76.06; H, 5.16. Found: C, 76.28; H, 5.14.

3.1.4. 2,2-Bis(2,4-dimethoxyphenyl)-3*H*-naphtho[2,1-*b*]pyran (4). Yield: 23%. Mp: 94–95 °C. ^{1}H NMR: δ 2.77 (s, 6H), 2.84 (s, 6H), 6.45 (d, 1H, J=6.8 Hz), 7.00–7.11 (m, 12H), 7.91 (d, 1H, J=5.8 Hz). IR (KBr): 1608, 1501 (C=C) cm^{-1}. EIMS: m/z 455 (M^+). Anal. Calcd for $C_{29}H_{26}O_5$: C, 76.65; H, 5.73. Found: C, 76.43; H, 5.72.

3.1.5. 2,2-Bis(3-fluoro-4-methoxyphenyl)-3*H*-naphtho[2,1-*b*]pyran (5). Yield: 41%. Mp: 132–134 °C. ^{1}H NMR: δ 3.85 (s, 6H), 6.12 (d, 1H, J=6.4 Hz), 6.96–7.71 (m, 12H), 7.95 (d, 1H, J=5.4 Hz). IR (KBr): 1621, 1514 (C=C) cm^{-1}. EIMS: m/z 431 (M^+). Anal. Calcd for $C_{27}H_{20}F_2O_3$: C, 75.34; H, 4.65. Found: C, 75.20; H, 4.64.

3.1.6. 2,2-Bis(3-chloro-4-methoxyphenyl)-3*H*-naphtho[2,1-*b*]pyran (6). Yield: 32%. Mp: 107–108 °C. ^{1}H NMR: δ 3.84 (s, 6H), 6.11 (d, 1H, J=9.8 Hz), 6.86–7.68 (m, 12H), 7.94 (d, 1H, J=8.4 Hz). IR (KBr): 1631, 1498 (C=C) cm^{-1}. EIMS: m/z 463 (M^+). Anal. Calcd for $C_{27}H_{20}O_3Cl_2$: C, 69.98; H, 4.32. Found: C, 69.96; H, 4.31.

3.2. Preparation of thin polymer films

To 60 mL of toluene, 10 g of the polymer was added and stirred until completely dissolved into transparent liquid by heating. Then a specified amount (weight percent loading) of **1**–**6** was added to the polymer solution and stirred well to mix. This solution was poured into a Petri dish and kept in a dark room. After complete evaporation of the solvent, the dish was baked in an oven at 60 °C for 20 min. The film was then peeled off from the dish. The resulting films were kept in a dark room.

Acknowledgments

Financial supports from the National Natural Science Foundation of China (Nos. 20490210 and 20372039) and N&T Joint Academy of China are gratefully acknowledged.

References and notes

1. Berkovic, G.; Krongauz, V.; Weiss, V. *Chem. Rev.* **2000**, *100*, 1741–1754.
2. Willner, I. *Acc. Chem. Res.* **1997**, *30*, 347–356.
3. Van Gemert, B. *Organic Photochromic and Thermochromic Compounds*; Crano, J. C., Guglielmetti, R. J., Eds.; Plenum: New York, NY, 1999; Vol. 1, pp 111–140, Chapter 3.
4. Balzani, V.; Credi, A.; Raymo, F. M.; Stoddart, J. F. *Angew. Chem., Int. Ed.* **2000**, *39*, 3348–3391.
5. Nakatani, K.; Delaire, J. A. *Chem. Mater.* **1997**, *9*, 2682–2684.
6. Delaire, J. A.; Nakatani, K. *Chem. Rev.* **2000**, *100*, 1817–1846.
7. Ortica, F.; Levi, D.; Brun, P.; Guglielmetti, R.; Mazzucato, U.; Facaro, G. *J. Photochem. Photobiol., A* **2001**, *139*, 133–141.
8. Ortica, F.; Levi, D.; Brun, P.; Guglielmetti, R.; Mazzucato, U.; Favaro, G. *J. Photochem. Photobiol., A* **2001**, *138*, 123–128.
9. Kumar, A.; Van Gemert, B.; Knowles, D. B. *Mol. Cryst. Liq. Cryst.* **2000**, *344*, 217–222.
10. Van Gemert, B.; Bergoni, M. P. U.S. Patent 5,066,818, 1991; Knowles, D. B. U.S. Patent 5,238,981, 1993.
11. Gabbutt, C. D.; Heron, B. M.; Instone, A. C.; Horton, P. N.; Hursthouse, M. B. *Tetrahedron* **2005**, *61*, 463–471.
12. Tan, T. F.; Fu, Y. F.; Han, J.; Pang, M. L.; Meng, J. B. *J. Mol. Struct.* **2005**, *743*, 157–162.
13. Aldoshin, S.; Chuev, I.; Filipenko, O.; Lokshin, V.; Samat, A.; Pepe, G. *Z. Kristallogr. New Cryst. Struct.* **1998**, *213*, 568–572.
14. Biryukov, B. P.; Unkovskii, B. V. *Kristallokhimiya* (*Crystal Chemistry*) **1974**, *29*, 110–115.
15. Gabbutt, C. D.; Gelbrich, T.; Hepworth, J. D.; Heron, B. M.; Hursthouse, M. B.; Partington, S. M. *Dyes Pigments* **2002**, *54*, 79–93.
16. Row, T. N. G. *Coord. Chem. Rev.* **1999**, *183*, 81–100.
17. Li, X. L.; Li, J. L.; Wang, Y. M.; Matsuura, T.; Meng, J. B. *J. Photochem. Photobiol., A* **2004**, *161*, 201–213.
18. Barnes, C. S.; Strong, M. I. *Tetrahedron* **1963**, *19*, 839–847.
19. Livingstone, R.; Miller, D.; Morris, S. *J. Chem. Soc.* **1960**, 5148–5152.
20. Cottam, J.; Livingstone, R. *J. Chem. Soc.* **1964**, 5228–5231.